

New phosphate glasses containing industrial waste and their applications for building engineering

C.L. Justino de Lima ^a, F.A. Veer ^b, O. Çopuroğlu ^a, R. Nijse ^{a, b}

Delft University of Technology, the Netherlands

^a Department of materials, mechanics, management & design (3Md),

^b Department of Architectural Engineering & Technology

Despite a large number of products developed from waste materials, most of them consist of non-transparent applications, partly because it is a challenge to get transparent materials at reasonable temperatures from these waste products. In this work, we produced transparent glass samples incorporating slag and fly ash into a phosphate glass matrix. The compositions were adjusted in order to circumvent typical drawbacks of phosphate glasses: a high thermal expansion coefficient and low chemical durability. The use of phosphate as a glass former, instead of silicate, is a remarkable innovation, and according to the knowledge of the authors, no other work reports its utilization for building engineering purposes. These novel glasses incorporate amounts up to 35% (in weight) of blast furnace slag or fly ash. Thermal, structural and mechanical characterization were performed. The glasses possess a low melting temperature in relation to the standard soda-lime and borosilicate glasses, melting in temperatures between 1100°C and 1350°C. This drastic reduction of the melting temperature allows to save energy during the manufacturing process. Furthermore, the valorization of materials that would otherwise have been previously discarded reduces costs and gas emission. It contributes to fill a current appeal for a more sustainable glass manufacturing process.

Keywords: Phosphate glass, fly ash, slag, industrial waste, recycling, glass

1 Introduction

The utilization of industrial waste materials in manufacturing building materials has increased considerably due to its increasing production and huge environmental problems caused by its disposal. Expanding populations, urbanization and increased wealth are

ramping up the global production of solid waste. Factors like population and per capita gross domestic product (GDP) are used to measure the total global municipal solid waste (MSW) production (Hoornweg et al. 2015). Some predictions about the world population suggest that the population will reach the highest point during this century. The waste production rates per capita usually grow with wealth, despite the fact that there is a tendency toward anti-materialism in the wealthiest countries. The junction of these aspects points to a scenario in which over the next decades the global waste generation will probably also peak (Hoornweg et al. 2015).

Fly ash is a by-product from burning pulverized coal in electric power generating plants, which is used in Portland Cement Concrete (PCC) pavement, paving roads, among others. Disposal of fly ash is becoming an expanding economic and environmental burden. For this reason, there is a current interest in looking for different applications for fly ash, other than the cement and construction industry (Zhang et al. 2007).

Steel slag is a mixture of metal oxides and silicon dioxide, which can include metal sulphide along with metal in the elemental form. Steel slag output consists of approximately 20% by mass of the crude steel output. In 2014, the global slag production was 250 Mt from the 1.6 bn tonnes of steel production (Dhoble et al. 2018). Slag is becoming value-added engineering material and utilized to develop materials like ceramics. New low-cost ceramics, without traditional fluxes and 30, 50 and 70% blast furnace slag were already synthesized at temperatures between 1200 and 1220 °C. The obtained samples presented good degrees of sintering and mechanical properties, which outperform the properties of the conventional building and tiling materials (Karamanova et al. 2011).

Despite a large number of products developed from waste materials, most of them consist of non-transparent materials, partly because it is a challenge to get transparent materials at reasonable temperatures from these waste products. Slag and fly ash contain many elements that are also present in typical glass formulas. For instance, the elements found in higher amounts in the compositions of standard silicate glasses are SiO₂, Na₂O, CaO, K₂O, MgO, Al₂O₃, Fe₂O₃ (Zschimmer, 2013). All those elements are found both in slag and in fly ash compositions. The compositions of blast furnace slag and fly ash are listed in Table 1. They are expressed as a function of the concentrations of silicon dioxide (SiO₂), aluminium oxide (Al₂O₃), calcium oxide (CaO), magnesium oxide (MgO), iron (III) oxide (Fe₂O₃),

Sulfur trioxide (SO₃), Sodium oxide (Na₂O), Potassium oxide (K₂O), Titanium dioxide (TiO₂) and Phosphorus pentoxide (P₂O₅). Some of those elements are highly refractory and their presence in complex compositions means they are highly likely to crystallize and have high working temperatures. However, glass is a material that allows large amounts of various elements in solution, being suitable to assimilate complex materials in its compositions.

Table 1: Chemical compositions of fly ash (FA) and blast furnace slag (BFS) deduced from X-ray fluorescence and expressed in mass%

| | SiO ₂ | Al ₂ O ₃ | CaO | MgO | Fe ₂ O ₃ | SO ₃ | Na ₂ O | K ₂ O | TiO ₂ | P ₂ O ₅ | L.O.I. |
|-----|------------------|--------------------------------|-------|------|--------------------------------|-----------------|-------------------|------------------|------------------|-------------------------------|--------|
| BFS | 34.40 | 11.53 | 39.17 | 7.81 | 1.42 | 1.6 | 0.23 | 0.58 | - | - | 1.15 |
| FA | 54.28 | 23.32 | 4.23 | 1.62 | 8.01 | 0.64 | 0.85 | 1.97 | 1.23 | 0.54 | 3.37 |

The materials listed in Table 1 had their structures analyzed by X-ray diffraction (XRD). The diffractogram of the slag is presented in Figure 1. The identified crystalline phase is the Quartz (SiO₂), but the sample is mostly amorphous.

The X-ray diffraction pattern of fly ash is presented in Figure 2. Besides the compound quartz, also identified in the slag, the mullite (3Al₂O₃.2SiO₂) was identified in the fly ash. It can be explained by the high concentration of Al₂O₃ in the composition of the fly ash. As illustrated in Table 1, Al₂O₃ corresponds to 23.32% of the mass of fly ash, while for the slag it consists of only 11.53% of the mass.

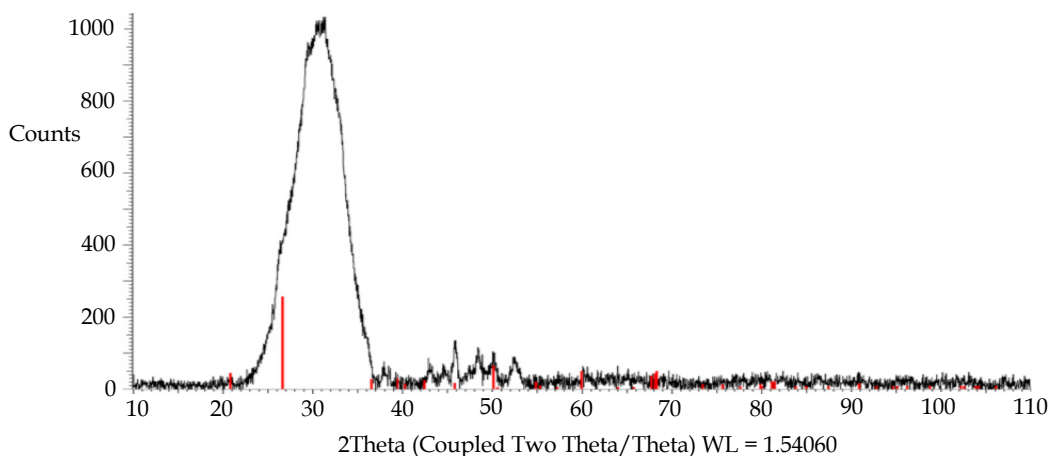


Figure 1: X-ray diffraction pattern of slag after background subtraction. The red sticks give the peak positions and intensities of the crystalline phase identified as SiO₂ quartz.

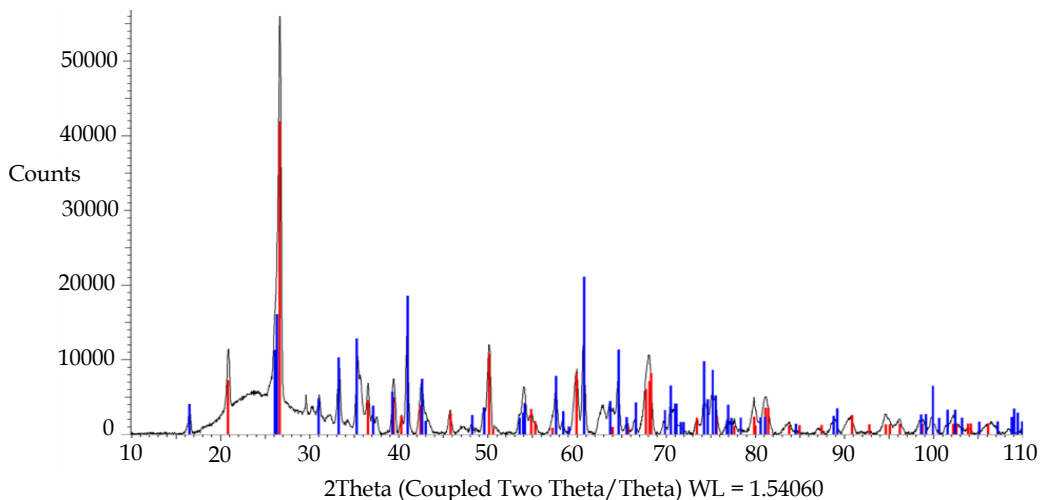


Figure 2: X-ray diffraction pattern of fly ash after background subtraction. The red sticks give the peak positions and intensities of the crystalline phase identified as SiO_2 , quartz. The blue sticks give the peak positions and intensities of the crystalline phase identified as $3\text{Al}_2\text{O}_3 \cdot 2\text{SiO}_2$, mullite.

In this work, we aimed to create new glass recipes incorporating waste materials into their compositions. Furthermore, we aim to create transparent materials at relatively low working temperatures. To reach these conditions, the elements, as well as the melting conditions, were optimized. The mechanical and thermal properties of the samples were measured and compared to the standard borosilicate and soda-lime glasses.

2 Methods

Almost the totality of the periodic table could hypothetically be incorporated into the glass. Consequently, choosing random elements to prepare glass is not an efficient option. The many possible combinations could lead to diverse properties far from the expected ones. Two main methodologies are currently used for glass production. The so-called “cook and look” technique has been used for a long time. Via this technique, a starting composition is developed based on available data, compositions previously reported and intuition. This composition is experimentally prepared at the laboratory, and its properties are characterized and measured. The determined properties are compared with the desired ones; based on the difference, the researcher develops more samples in an attempt to fine-tune the composition and get closer to the target (Mauro, 2017). On the one hand, this technique has already yielded in fruitful results which originated many commercial

products. On the other hand, the large number of tested compositions can be expensive and results in a long process, especially if the choice of the starting composition is made without careful criteria and its properties are very far from the target.

Another technique is based on the use of predictive modelling tools to facilitate the design of new glass compositions. Quantitatively precise models have already been developed for different properties. However, each model is only appropriate to solve a certain type of problem. There is still no model that is able to address every property simultaneously (Mauro 2017). Topological constraint theory and atomistic simulations are examples of cases in which precise predictions of properties are made based on the chemical makeup of the glass. However, as the glass is a non-crystalline material, its atomic positions are not known with absolute certainty. They should be described using probability distribution functions, which makes the predictions more complex. An ideal application of this approach would require modellers working closely with experimentalists. Although the use of predictive modelling becomes each day more unavoidable the selection and implementation of the models is still a long process that requires interdisciplinary work. Collaboration among professionals skilled in chemistry, physics, and materials can facilitate the selection and implementation of models.

In this study we used the first technique, starting from an initial glass composition. The elements were weighted using an analytical balance and ground using a ceramic mortar. This mixture was transferred to a platinum crucible and melted for 1 hour. Melting temperatures ranged from 1100°C to 1350°C, depending on the glass composition. The melted mixtures were poured into a stainless steel mould preheated to around 450°C and were annealed at this temperature for 3 hours before cooling to room temperature inside the furnace. These glass samples were then ground and polished. The steps of this process are illustrated in Figure 3.

Phosphate was used as a glass former, being obtained from the element KH_2PO_4 (potassium dihydrogen phosphate), which in high temperatures transforms into KPO_3 (potassium metaphosphate) and H_2O . Aluminium oxide (Al_2O_3) was added in order to improve the chemical durability of the glasses. Fly ash and blast furnace slag were also incorporated in amounts as high as possible. These waste materials were used in the powder form, and they can be observed in Figure 4.

3 Results

Characterization techniques like thermal analysis, nanoindentation, X-ray fluorescence and X-ray diffraction were used to determine the properties of the developed compositions. The process of development of the samples, as well as the results obtained from the characterization techniques, are presented in this section.

The choice of the element used as glass former is the first step to design a glass composition. Phosphate glasses possess relatively low working temperatures, low liquidus viscosity, high UV transparency and high solubility for other glass modifiers or intermediaries. Pure P_2O_5 melts around $562^\circ C$ (Rumble, 2018). One of their major drawbacks is that these glasses are usually hygroscopic and not stable under room

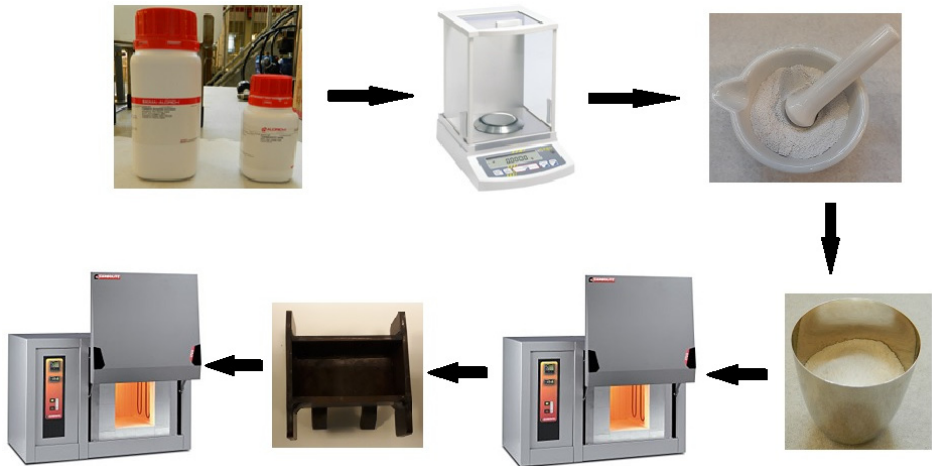


Figure 3: Scheme of the glass samples production: preparation of the batch, melting, quenching and annealing



Figure 4: The raw waste materials, fly ash and slag

atmosphere. However, in the last decades, the compositions were adjusted and phosphate glasses with high stability against devitrification were developed.

For this reason, phosphate was used as a glass former in this study. The element KPO_3 was chosen as the phosphate source. In high temperatures, KPO_3 can be obtained from the decomposition of the element KH_2PO_4 (Potassium phosphate monobasic), as presented in Equation 1. The element KH_2PO_4 , in its turn, results from the synthesis of the elements K_2O (Potassium Oxide), P_2O_5 (Phosphorus pentoxide) and H_2O , as shown in Equation 2.



The first melting attempts aimed to obtain samples from a binary mixture of KPO_3 and slag or fly ash. However, they produced non-transparent materials. The addition of Aluminum oxide (Al_2O_3) yielded transparent glass samples. Boron trioxide (B_2O_3) was added to some samples as an attempt to decrease the thermal expansion coefficient of the glasses.

The composition of some samples was checked by XRF and compared with the expected composition. Samples containing B_2O_3 could not have their compositions analyzed because boron is not measured by XRF. The expected compositions were calculated based on the deduced compositions of fly ash and slag, already presented in Table 1. The results presented in Table 1 include the Loss on ignition (LOI) value, which is related to the percentage of weight that a material loses on firing. The LOI values were discarded for the estimations of the compositions of the glasses. Due to the fact that the wastes are not homogeneous materials, differences between the theoretical and the actual compositions were already predicted. The compositions of the samples $60KPO_3$ - $25FA$ - $15Al_2O_3$ and $60KPO_3$ - $20Slag$ - $20Al_2O_3$ were analyzed by XRF and the results are presented in Tables 2 and 3. Both samples present a significant difference between the theoretical and the actual compositions.

Considering pure reagents, with a purity of at least 99%, an estimation was made to calculate the costs of the glass containing wastes in relation to commercial glasses. Slag and fly ashes were considered materials free of costs, as they are by-products. Therefore, the prices decrease with the increasing amount of wastes, which substitute other elements.

Table 2: Theoretical and actual compositions of the sample 60KPO₃-25FA-15Al₂O₃

| Compound | Theoretical composition wt (%) | Actual composition wt (%) | Absolute error wt (%) |
|--------------------------------|-----------------------------------|------------------------------|--------------------------|
| P ₂ O ₅ | 36.5 | 38.4 | 0.1 |
| K ₂ O | 24.63 | 19.97 | 0.1 |
| Al ₂ O ₃ | 21 | 22.22 | 0.1 |
| SiO ₂ | 13.69 | 15.22 | 0.1 |
| CaO | 1.07 | 1.1 | 0.03 |
| MgO | 0.4 | 0.41 | 0.02 |
| Fe ₂ O ₃ | 2.02 | 1.72 | 0.04 |
| SO ₃ | 0.16 | 0.03 | 0.005 |
| Na ₂ O | 0.21 | 0.39 | 0.02 |
| TiO ₂ | 0.3 | 0.24 | 0.01 |

Table 3: Theoretical and actual compositions of the sample 60KPO₃-20Slag-20Al₂O₃

| Compound | Theoretical composition wt (%) | Actual composition wt (%) | Absolute error wt (%) |
|--------------------------------|-----------------------------------|------------------------------|--------------------------|
| P ₂ O ₅ | 36.3 | 41.69 | 0.1 |
| K ₂ O | 24.2 | 22.4 | 0.1 |
| Al ₂ O ₃ | 22.44 | 18.69 | 0.1 |
| SiO ₂ | 6.94 | 7.77 | 0.08 |
| CaO | 7.88 | 7.01 | 0.08 |
| MgO | 1.57 | 1.64 | 0.04 |
| Fe ₂ O ₃ | 0.28 | 0.11 | 0.01 |
| SO ₃ | 0.32 | 0.12 | 0.01 |
| Na ₂ O | 0.05 | 0.11 | 0.01 |

Table 4: The estimated price of some compositions made by high purity elements

| Composition | Price |
|--|-----------|
| 73SiO ₂ -14Na ₂ O-9CaO-4MgO (Soda-lime) | € 166 /kg |
| 80SiO ₂ -13B ₂ O ₃ -4Na ₂ O ₃ -3Al ₂ O ₃ (Borosilicate) | € 180 /kg |
| 60KPO ₃ -30FA-10Al ₂ O ₃ | € 63 /kg |
| 75KPO ₃ -12.5Slag-12.5Al ₂ O ₃ | € 78 /kg |
| 40KPO ₃ -25FA-15Al ₂ O ₃ -20B ₂ O ₃ | € 93 /kg |

Table 4 points that the cost of the commercial glasses is significantly higher than the cost of the glasses containing waste.

In the past, the low chemical durability of phosphate glasses limited their applications. The term “chemical durability” has been used commonly to indicate the resistance offered by a glass towards attack by aqueous solutions and atmospheric agents (Paul, 1982). Nowadays, it is known that the addition of some elements on the phosphate glasses is able to overcome this drawback, achieving a high chemical durability. For this reason, it is important to measure the chemical durability of the samples and how the introduction of different elements affect this property.

Existing literature points out that the incorporation of Al_2O_3 is linked to higher chemical durability in the samples (Inaba, 2016). This relation was reinforced by the water resistance tests conducted in this study. There is no absolute measure of chemical durability and glasses are generally graded relative to one another after subjecting them to similar experimental conditions; the nature of the experiment usually determines the relative order. On the one hand, they can be accelerated tests, which are performed in the laboratory under a controlled environment and possibly do not represent real conditions. On the other hand, they can be long-term tests that due to the duration can be difficult to keep continuity and still have to be extrapolated. Long-term tests are generally conducted under a less controlled environment, but they may be more representative of real conditions. Other test conditions can also change, like the protocols (static or dynamic) and the sample preparation; the glass can be tested as a whole article or as a powder. The MCC-1 static test is an example of a patterned test. It was developed as a standard leach test for nuclear waste forms and tests monolithic samples kept in PFA Teflon vessels under leaching solutions (deionised water, reference silicate solution or reference brine) during 28 days at 90°C, 70°C or 40°C (Strachan et al., 1982). In the current study, we tested the samples keeping them statically, under demineralized water and ambient temperature in plastic vessels during 30 days.

Concentrations of Al_2O_3 lower than 12.5% cannot improve the chemical durability. It was already reported that binary or ternary phosphate samples with a very low Al_2O_3 content present a very low durability. After 24 hours under demineralized water all the tested samples, with concentrations of Al_2O_3 lower than 12.5%, presented a significant loss in their initial mass (de Lima et al. 2018). Therefore, the Al_2O_3 was added to the samples in

concentrations between 12.5% and 20%. The samples listed in table 5 were kept under demineralized water for 30 days without any mass loss.

The color of a glass is affected by various factors, like coordination number, variation in redox states and melting temperature. For this reason, the obtained glasses present a wide range of colorations.

Table 5: Compositions in weight of Series 2 samples that remained under demineralized water for 30 days with no mass loss

| KPO ₃ | Fly ash | Slag | Al ₂ O ₃ |
|------------------|---------|------|--------------------------------|
| 60 | 25 | - | 15 |
| 70 | 15 | - | 15 |
| 75 | 12.5 | - | 12.5 |
| 60 | 20 | - | 20 |
| 55 | 35 | - | 10 |
| 65 | 20 | - | 15 |
| 60 | 30 | - | 10 |
| 70 | - | 15 | 15 |
| 60 | - | 20 | 20 |
| 65 | - | 17.5 | 17.5 |

For the samples containing slag, we obtained transparent materials with a maximum concentration of 15% of this waste material. The samples consisting of 12.5% of slag show blue coloration, while the ones consisting of 15% have amber coloration. It is also possible to obtain samples with a higher concentration of slag; however, they are not transparent. All the samples are illustrated in Figure 5.

The samples containing slag were very sensitive to some melting conditions and small variations in the compositions. Phase separations were observed in those samples, while the samples containing fly ash retained homogeneity after all the tests. The sample consisting of 12.5% slag exhibits different colorations depending on the temperature at which is melted. Melted at 1150°C, the sample shows a homogeneous blue coloration. At 1250°C it is heterogeneous and reveals two different patterns of coloration, blue and transparent. At 1350°C the sample is homogeneous and transparent. The visual aspects of the sample melted at the three temperatures are found in Figure 6. Due to the complexity

to describe multi-component systems, only the use of techniques as NMR and Raman could explain in details the reasons behind the color variation of these samples.

The sample consisting of 15% slag presents homogeneity and amber coloration. Tests were made adding Boron oxide (B_2O_3) at the composition, in an attempt to decrease its thermal expansion. The introduction of 10% of B_2O_3 modifies the visual aspect of the sample, which becomes heterogeneous and transparent with light yellow areas. Further addition of 10% B_2O_3 , totalizing 20%, generates two phases, one transparent and one blue. The three samples are shown in Figure 7.

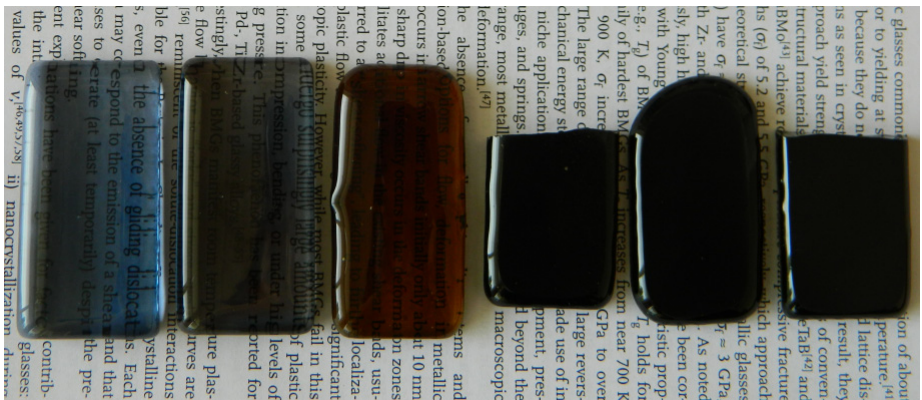


Figure 5: The samples containing slag. From the left to the right: $77.5KPO_3-10Slag-12.5Al_2O_3$, $75KPO_3-12.5Slag-12.5Al_2O_3$, $70KPO_3-15Slag-15Al_2O_3$, $65KPO_3-17.5Slag-17.5Al_2O_3$, $65KPO_3-20Slag-15Al_2O_3$, $60KPO_3-20Slag-20Al_2O_3$.



Figure 6: Samples consisting of 12.5% slag melted at different temperatures: 1150°C, 1250°C, and 1350°C, respectively



Figure 7: Samples consisting of 15% slag, without the addition of B_2O_3 , with the addition of 10% B_2O_3 and 20% B_2O_3 , respectively

For the samples containing fly ash, samples with a maximum concentration of 35% of fly ash were obtained. The samples consisting of 35% fly ash show dark green coloration and were produced at 1350°C. The samples consisting of 15% fly ash are yellow and can be produced at lower temperatures (1100°C). The samples become darker for higher concentrations of fly ash, as illustrated in Figure 8. No tests were conducted for fly ash concentrations higher than 35%. It is probably possible to produce glass samples at temperatures higher than that. However, these temperatures would be higher than 1400°C and the samples would present a very dark coloration, which is not useful for the purposes of this work.



Figure 8: The samples containing fly ash. From the left to the right: $75\text{KPO}_3\text{-}12.5\text{FA}\text{-}12.5\text{Al}_2\text{O}_3$, $70\text{KPO}_3\text{-}15\text{FA}\text{-}15\text{Al}_2\text{O}_3$, $65\text{KPO}_3\text{-}20\text{FA}\text{-}15\text{Al}_2\text{O}_3$, $60\text{KPO}_3\text{-}20\text{FA}\text{-}20\text{Al}_2\text{O}_3$, $60\text{KPO}_3\text{-}25\text{FA}\text{-}15\text{Al}_2\text{O}_3$, $60\text{KPO}_3\text{-}30\text{FA}\text{-}10\text{Al}_2\text{O}_3$, $55\text{KPO}_3\text{-}35\text{FA}\text{-}10\text{Al}_2\text{O}_3$

In order to confirm the vitreous structure, the samples containing the most waste materials had their structures analyzed by X-ray diffraction (XRD). This analysis confirmed the amorphous character of the samples, even the darkest ones, because they exhibit the large bump characteristic of amorphous materials, as can be observed in their XRD patterns in Figures 9 and 10.

The glass transition region was detected using differential scanning calorimetry (DSC) that is based on the heat property of materials. The first phenomenon to appear on a DSC curve of a glass is the glass transition (T_g), which corresponds to a baseline change. Next, one can note exothermic peaks, relative to crystallization and an endothermic peak, which may be related to the melting of the crystalline phase (T_m). The onset crystallization temperature is called T_x , while the peak crystallization temperature is known as T_c .

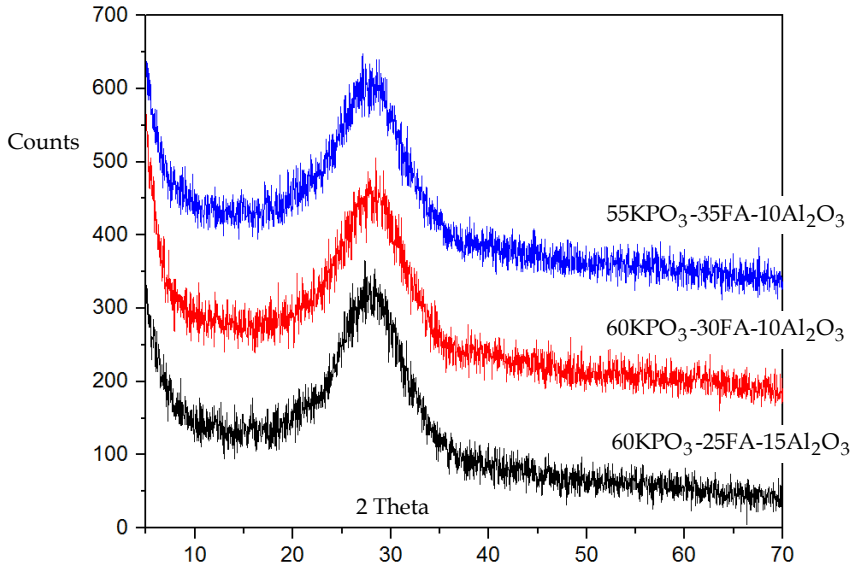


Figure 9: X-ray pattern of the samples with a high concentration of fly ash

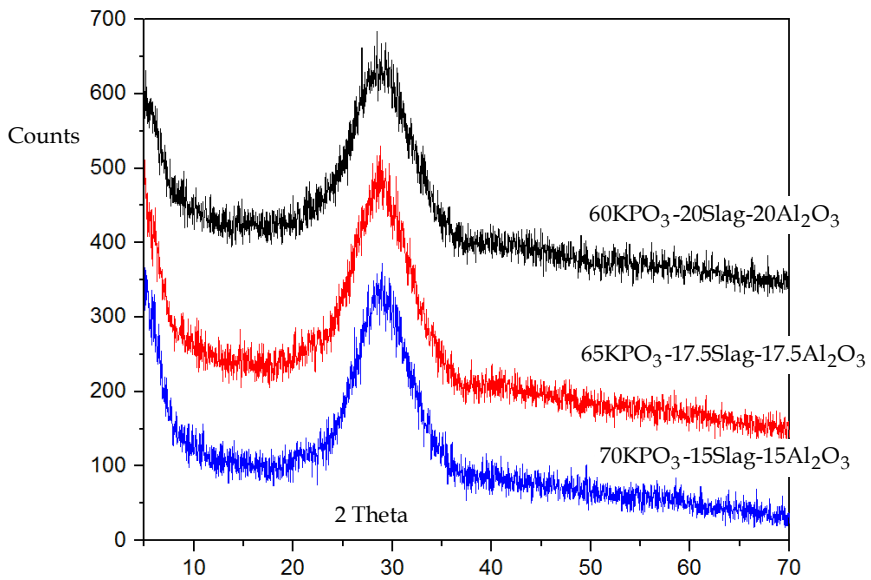


Figure 10: X-ray pattern of the samples with a high concentration of slag

The glasses consisting of waste materials were melted at a minimum temperature of 1100°C, and a maximum of 1350°C. Figure 11 shows the characteristic temperatures for one sample consisting of 12.5% of slag and a sample consisting of 20% of slag in relation to a commercial borosilicate glass. While in the 12.5% slag sample the range of glass-liquid transition temperatures is around 443°C, the T_g of the sample containing 20% of slag cannot be localized with precision, but a transformation seems to occur around 490°C. For the commercial glass, it is around 545°C. Both areas are circled in Figure 11.

Crystallization peaks are found for all the samples. The glasses consisting of slag present a peak with a higher intensity, around 638°C for the sample with 12.5% of slag while the first crystallization peak of the sample containing 20% of slag is around 665°C. It was expected due to the high tendency of crystallization of waste materials, which are rich in various oxides.

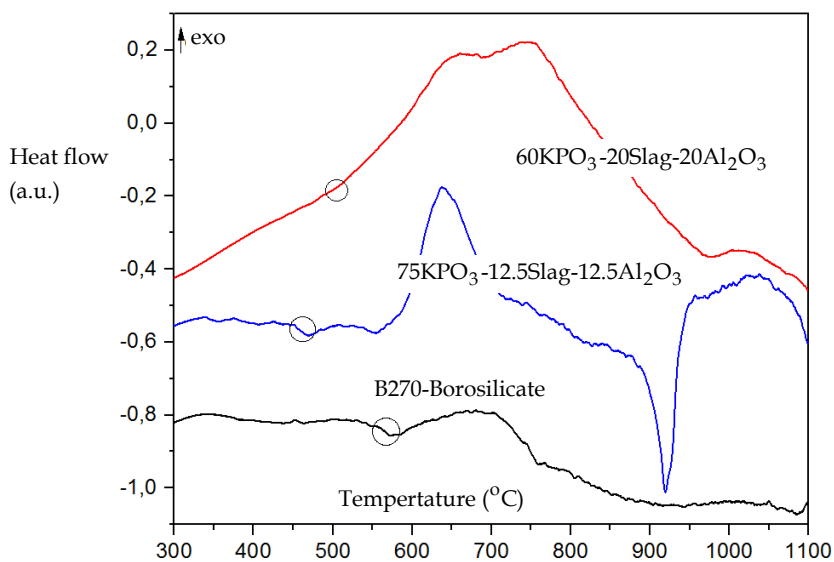


Figure 11: Thermal analysis curves of a borosilicate glass and glasses containing slag. Glass transition regions are highlighted.

For the glasses containing fly ash, a glass transition region can be detected for both samples, as observed in Figure 12. The glass containing 12.5% of fly ash has a T_g around 412°C, and the one containing 30% of fly ash has a T_g around 465°C. It highlights the fact that the T_g increases with the amount of waste incorporated in the composition.

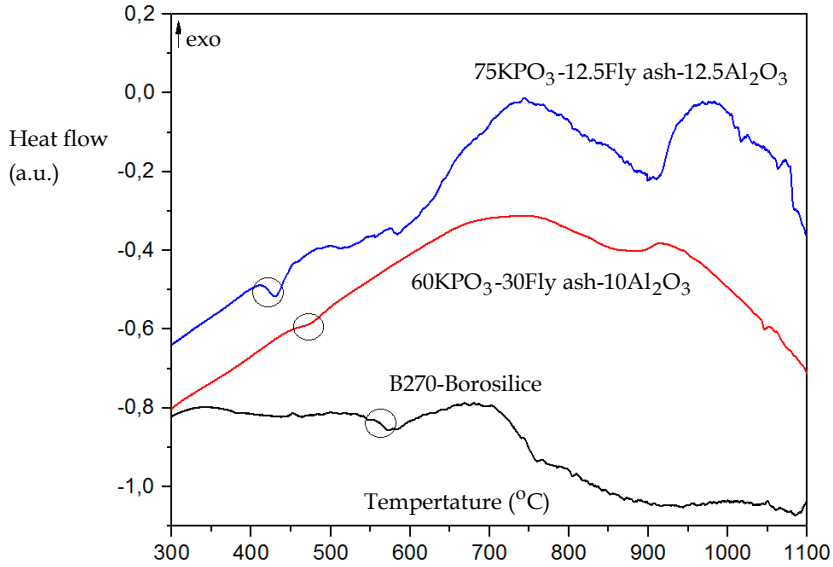


Figure 12: Thermal analysis curves of a borosilicate glass and glasses containing fly ash. Glass transition regions are highlighted.

The glasses had some mechanical properties analyzed. The elastic modulus and the hardness were measured via the nanoindentation technique.

There is a trend of increasing both properties with amounts of slag and Al_2O_3 . The results of the samples consisting of slag are shown in Table 6, and the results of the samples consisting of fly ash are presented in Table 7.

Table 6: Average elastic modulus and hardness of the samples consisting of slag

| Sample | Composition | Average E (GPa) | Average H (GPa) |
|--------|--|-----------------|-----------------|
| 1 | 70KPO ₃ -15Slag-15Al ₂ O ₃ | 43.7 | 4.19 |
| 2 | 50KPO ₃ -20B ₂ O ₃ -15Slag-15Al ₂ O ₃ | 45.5 | 4.67 |
| 3 | 65KPO ₃ -17.5Slag-17.5Al ₂ O ₃ | 46.7 | 4.59 |
| 4 | 65KPO ₃ -20Slag-15Al ₂ O ₃ | 49.2 | 4.85 |
| 5 | 60KPO ₃ -20Slag-20Al ₂ O ₃ | 52.6 | 5.14 |

Considering samples with a same amount of KPO₃, the addition of waste is more effective to increase both properties than the addition of Al₂O₃. It can be observed comparing samples 3 and 4 from Table 6 or samples 1 and 2 from Table 7. Comparing Table 6 and

Table 7 it is noticeable that glasses consisting of slag possess higher elastic modulus and hardness than the glasses consisting of fly ash.

Table 7: Average elastic modulus and hardness of the samples consisting of fly ash

| Sample | Composition | Average E (GPa) | Average H (GPa) |
|--------|--|-------------------|-------------------|
| 1 | 60KPO ₃ -20FA-20Al ₂ O ₃ | 41.6 | 3.94 |
| 2 | 60KPO ₃ -25FA-15Al ₂ O ₃ | 42.3 | 3.99 |
| 3 | 55KPO ₃ -35FA-10Al ₂ O ₃ | 43.5 | 4.18 |
| 4 | 60KPO ₃ -30FA-10Al ₂ O ₃ | 45.2 | 4.56 |
| 5 | 40KPO ₃ -20B ₂ O ₃ -25FA-15Al ₂ O ₃ | 48.4 | 5.02 |

4 Discussion

The Silicon oxide is the largest used glass former, due to its superior properties like the high chemical durability, low price and large availability. It is the main constituent of borosilicate and soda-lime glasses. However, new glass applications demand glasses with specific properties. In this work, we used phosphate as a network former, instead of silicate. As a result, the properties of these glasses differ from the properties of the glasses typically used in building engineering.

One of this properties is the chemical durability. The addition of Al₂O₃ proved to be a way to overcome the low chemical durability of the phosphate glasses. As an example of the low durability of the phosphates glasses, the reported compositions 54.5P₂O₅-20.5K₂O-20.5Cs₂O-4.5Al₂O₃ and 50P₂O₅-16.7Na₂O-16.7K₂O-16.7Cs₂O show a mass loss of 19.3% and 100%, respectively, when dipped in water at 18°C for only 1 hour (Inaba, 2016).

In contrast, samples developed in this study with a concentration of Al₂O₃ between 12.5% and 20% were kept under demineralized water for 30 days without any mass loss.

The high chemical durability of soda-lime glass is one of the reasons that explain its popularity, allowing the use of this glass in bottles, windows and other applications which require a high water resistance. Therefore, the achievement of a high water resistance by the phosphate glasses containing wastes was a fundamental step in order to develop a glass suitable for a wide range of applications.

The developed glasses present a variety of colors: amber, blue, green, transparent and yellow. As a general trend, the glasses become darker for higher amounts of waste. Other variations in color can arise from different melting temperatures in the case of the glasses containing slag. Further studies will be conducted in order to understand the origin of these different colorations. The fact that a composition is so susceptible to changes in melting conditions and to the introduction of further elements, generates glass with interesting and unique coloration. However, this is a drawback if we intend to manufacture glass on a commercial scale. The presence of impurities in the melting or the use of a furnace with a non-tightly-controlled temperature would produce glasses with undesirable properties. Considering this point, the manufacture of glasses containing fly ash is more beneficial than the ones containing slag.

Based on the results obtained from the characterization techniques, other properties of these phosphate glasses are summarized and compared to the properties of benchmark glasses in Table 8.

Table 8: The properties of the phosphate glasses containing wastes in relation to the properties of soda-lime and borosilicate glasses

| Property | Phosphate glasses containing waste | Soda-lime glass | Borosilicate glass |
|------------------------------|------------------------------------|-----------------|--------------------|
| Price | € 63-93/kg | € 166/kg | € 180/kg |
| Melting temperature | 1100 °C -1350 °C | 1675 °C | 1650 °C |
| Glass transition temperature | 443 °C - 490 °C | 572 °C | 545 °C |
| Elastic modulus | 41.6 GPa - 52.6 GPa | 74 GPa | 63 GPa |
| Hardness | 3.94 GPa - 5.15 GPa | 5.5 GPa | 6.4 GPa |

The addition of B_2O_3 increases the final price due to the price of this element. However, even with the addition of B_2O_3 , the final price of the phosphate glasses is still significantly lower than the price of the silicate glasses.

The glass transition temperature of the glasses containing wastes increases with the amount of waste incorporated in the composition. As a consequence, the melting temperature also increases. For the phosphate glasses, the melting temperature, which is presented in Table 8, corresponds to the temperature in which the viscosity of the liquid is low enough to be quenched from the crucible to the mould. For the benchmark glasses, the

exhibited melting temperatures are related to temperatures in which these glasses are industrially melted and possess a viscosity low enough to be moulded (de Jong, 1989). The melting temperatures of all the developed compositions are still low in relation to the melting temperature of borosilicate and soda-lime glasses, as shown in Table 8. The production of glasses with lower melting temperatures demands less energy, and, as a consequence, the environmental impact and manufacturing cost decrease.

It is noticeable that glasses consisting of slag possess higher elastic modulus and hardness than the glasses consisting of fly ash. The different compositions of the raw waste materials could be a possible explanation for this variation in the properties of the glasses containing wastes. The slag contains 39.17% of CaO (Calcium oxide), while the fly ash contains 4.23% of the same element. The hardness of a phosphate glass can increase with the CaO content due to densification (Rao et al. 2014). Furthermore, the CaO is easily crystallized, and it could explain the fact that materials consisting of slag can form glass in a shorter range of compositions than the ones consisting of fly ash.

All the produced glasses possess lower elastic modulus and hardness than the values presented for the standard silicate glasses (Chorfa et al. 2010).

The simultaneous achievement of high hardness and crack resistance is an important concern in glass science and technology. Crack-resistant glasses are able to release the stress without cracking, via atom displacements. It results in plastic deformation mainly by densification and, in some measure, by shear deformation. Due to their high molar volume and low atomic packing density, in these glasses atoms can easily be compacted by force. Moreover, crack-resistant glasses present low elastic moduli, between 60 and 70 GPa, and low Vickers hardness, around 5–6 GPa (Rosales-Sosa et. al, 2016). Despite some exceptions, it is assumed that “hard” and “crack-resistant” are not achieved at the same time in conventional oxide glasses because high packing density is a characteristic of hard glasses (Rosales-Sosa et. al, 2016).

For this reason, the fact that the glasses developed in this work possess low elastic moduli and hardness, when compared to standard glasses, leads to a hypothesis that they could present a higher crack resistance. Further measurements will be conducted in order to verify this hypothesis.

5 Applications and perspectives

Some of the new compositions developed at this work were chosen to be cast as glass bricks. Initial tests are being conducted using the “flowerpot method”, in order to evaluate the stability of these glasses against devitrification and their potential to be cast by a slow cooling process.

The “flowerpot” casting method is used for the feeding of the glass into the moulds. This method consists of the positioning of terracotta flowerpots filled with glass above the moulds. At forming temperatures the glass drops down through the flowerpot hole and fills the mould (Bristogianni et al. 2017). Traditionally, the flowerpots are filled with commercial glass. However, in our experiments, they are filled with the developed compositions, in the form of bulk (cullet) glass or raw materials. Testing to feed the mould with the material in two different forms, bulk glass and the raw batch powder, is important because the particle size can influence the melting process. Both forms are shown in Figure 13.

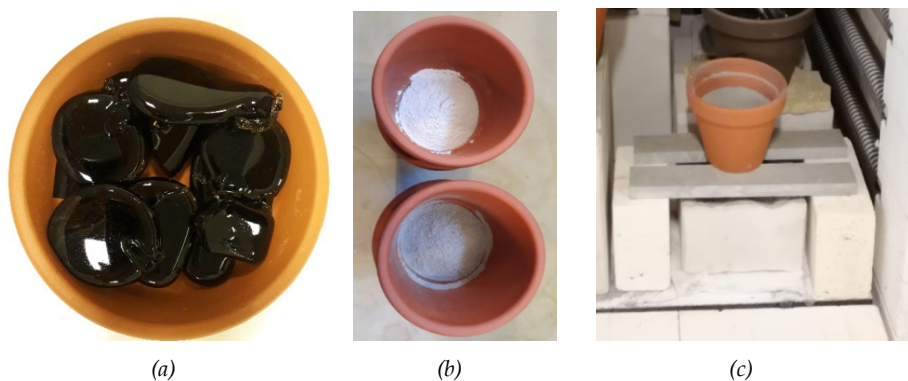


Figure 13: Terracotta flowerpots (a) filled with the bulk glass (b) filled with the raw batch materials: $60\text{KPO}_3\text{-}30\text{FA-}10\text{Al}_2\text{O}_3$ (grey powder) and $60\text{KPO}_3\text{-}20\text{slag-}20\text{Al}_2\text{O}_3$ (white powder) (c) filled with raw batch materials and above the mould, in the furnace.

Compared to a virgin (mined and processed) glass batch raw materials, the melting energy consumption of cullet is approximately 70–75%. Consolidated batch can provide advantages in the furnace such as decreased melting and refining times and increased batch thermal conductivity compared with unconsolidated batch materials (Deng et al. 2018). The efficiency of heat transfer through glass batch is an important factor affecting

the energy efficiency of glass manufacturing and product quality (Doi et al. 2018). The melting of glass batch raw materials can generate gas conduction, bubbles and can limit the heat transfer. Furthermore, the particles can behave as nucleating agents, promoting crystallization.

The flowerpot process has a slow cooling rate in relation to the traditional melt-quenching method. It is a kiln-casting method, where the melting, pouring and annealing of the glass takes place in the same kiln. The mould is kept inside the kiln at all stages. For this reason, a composition can form a glass when melted via the melt-quenching process but crystallize when the kiln-casting process is applied. One example of these different results is illustrated in Figure 14. The sample $60\text{KPO}_3\text{-}20\text{slag-}20\text{Al}_2\text{O}_3$ is a dark glass, which already had its amorphous structure confirmed by XRD in Figure 10 when produced via the melting-quenching process. However, it becomes a white solid when produced via the kiln-casting method. It was melted and cooled inside of the same pot. Melting from the batch raw materials at 970°C and cooled in a rate of around $2.66^\circ\text{C}/\text{minute}$.



Figure 14: The sample $60\text{KPO}_3\text{-}20\text{slag-}20\text{Al}_2\text{O}_3$ produced, respectively, via the melt-quenching and the kiln-casting method

The diffractogram of the sample made by the kiln-casting method is presented in Figure 15. A phase related to the Potassium Calcium Magnesium Phosphate $\text{Ca}_9\text{MgK}(\text{PO}_4)_7$ was identified. The presence of this phase could be related to the high amounts of CaO and MgO present in the composition of the slag. Both oxides act like network modifiers, which when added to a glass matrix can induce the crystallization.

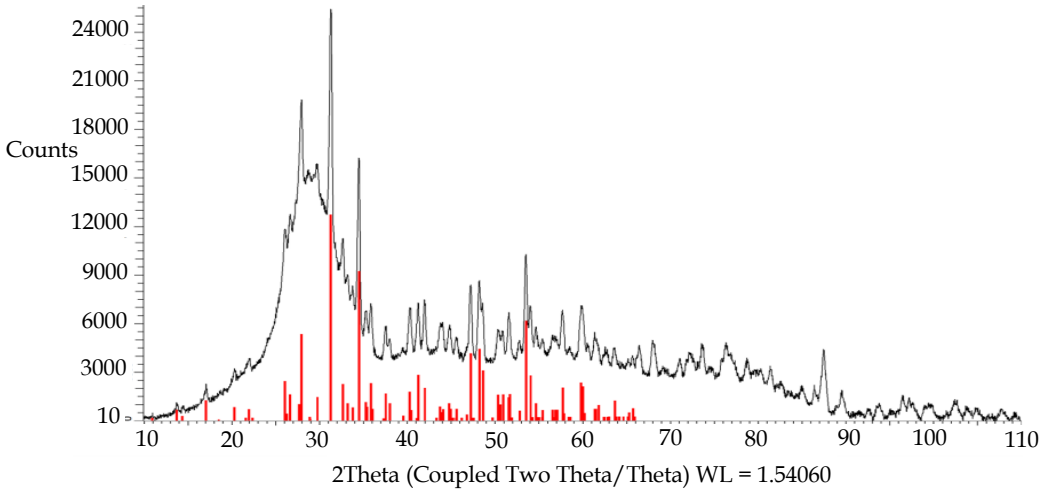


Figure 15; X-ray diffraction pattern of the sample $60\text{KPO}_3\text{-}20\text{slag-}20\text{Al}_2\text{O}_3$, produced by the kiln-casting method, after background subtraction. The red sticks give the peak positions and intensities of the crystalline phase identified as $\text{Ca}_9\text{MgK}(\text{PO}_4)_7$, Calcium Magnesium Phosphate.

High stability is required from the composition in order to prevent the crystallization upon the slow cooling. A sample consisting of $60\text{KPO}_3\text{-}30\text{FA-}10\text{Al}_2\text{O}_3$ was also melted from the batch raw materials at 970°C and cooled in a rate of around $2.66^\circ\text{C}/\text{minute}$, via the kiln-casting method. The visual aspect of this sample is glassy, similar to the same composition melted by the melt-quenching method, as pointed in Figure 16.



Figure 16: The sample $60\text{KPO}_3\text{-}30\text{FA-}10\text{Al}_2\text{O}_3$ produced, respectively, via the melt-quenching and the kiln-casting method

The XRD pattern of the sample produced by a fast cooling was already shown in Figure 9, and it is amorphous. Figure 17 shows the structure of the sample produced by slow cooling. The identified phase is related to quartz. However, the low intensity of the peaks points that the sample is essentially amorphous. The results of these tests are summarized in Table 9 and compared to the results obtained for benchmark glasses (Bristogianni et al., 2018).

Table 9: Conditions and results of the kiln-casting method applied to the phosphate glasses and to standard glasses

| Composition | Glass transition T_g | Melting temperature | Structure |
|---|---------------------------|------------------------|---|
| 60KPO ₃ -20slag-20Al ₂ O ₃ | 490°C | 970°C | Crystal, Ca ₉ MgK(PO ₄) ₇ |
| 60KPO ₃ -30FA-10Al ₂ O ₃ | 465°C | 970°C | Amorphous, but with peaks of low intensity related to Quartz. |
| Soda-lime-float (PPG Starphire) | 570°C | 1200°C | Amorphous, but with top surface crystallization. |
| Borosilicate (Schott- Duran) | 525°C | 1200°C | Amorphous, but with top surface crystallization. |

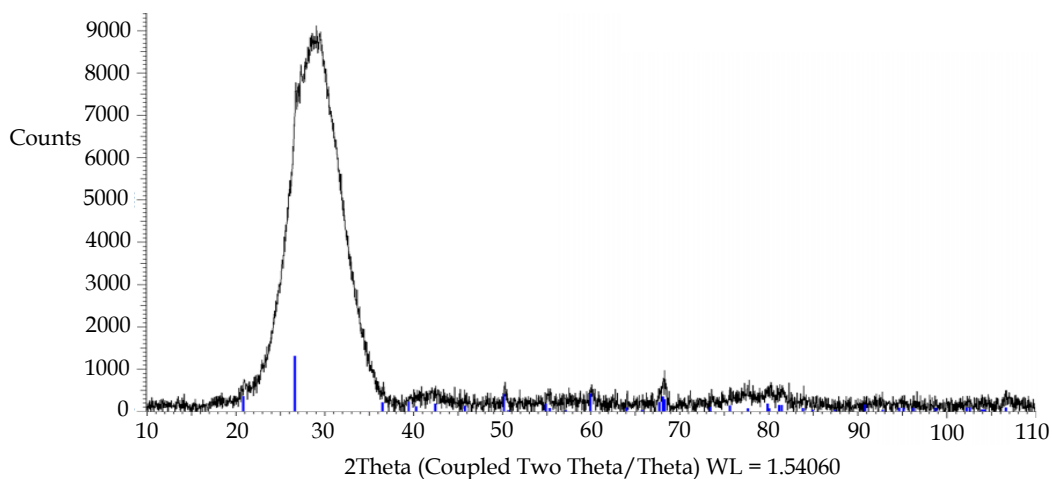


Figure 17: X-ray diffraction pattern of the sample 60KPO₃-30FA-10Al₂O₃, produced by the kiln-casting method, after background subtraction. The blue sticks give the peak positions and intensities of the crystalline phase identified as SiO₂, quartz

As observed in Table 9, the benchmark glasses possess higher glass transition temperatures than the phosphate glasses. Furthermore, they have a higher viscosity. For these reasons, the casting tests of these glasses were conducted in higher melting temperatures. The results demonstrate that the sample containing fly ash possesses a higher stability against devitrification than the sample containing slag. Moreover, this sample has a stability against devitrification comparable to the benchmark glasses. After the casting, both result in predominately amorphous materials.

6 Conclusions

In this work, we proved that it is possible to create new glass compositions using industrial waste. Due to the intrinsic properties of phosphate, the glasses produced at this work have a low melting temperature in relation to the standard soda-lime and borosilicate glasses. They melt in temperatures between 1100°C and 1350°C while the traditional glasses melt around 1650°C. This drastic reduction of the melting temperature allows to save energy during the manufacturing process. Furthermore, the valorization of materials that would otherwise have been previously discarded reduces costs and gas emission. The water resistance of the glasses was greatly improved with changes in the compositions, adding the wastes, which contain high amounts of oxides, and extra amounts of Al_2O_3 . Due to this combination, the compositions achieved high water resistance.

We produced materials consisting of up to 35% of fly ash, and 20% of slag and their vitreous structures were confirmed using X-ray diffraction. Nanoindentation points that it is possible to control the properties according to the amount of wastes and Al_2O_3 incorporated in the composition. There is a trend of increasing elastic modulus and hardness with amounts of slag, fly ash and Al_2O_3 . For the samples containing slag, the elastic modulus varies from 43.7 to 52.6 GPa, and the hardness from 4.19 to 5.14 GPa. For the samples containing fly ash, the elastic modulus ranges from 41.6 to 48.4 GPa, and the hardness from 3.94 to 5.02 GPa. The coloration of the samples varies depending on the composition and melting temperature. Besides to form glass in a larger range of compositions, the samples consisting of fly ash are also less susceptible to changes in melting conditions and to the introduction of further elements, and ash possess a higher stability against devitrification. Therefore, the manufacturing of glasses containing fly ash is more profitable than the ones containing slag.

Acknowledgements

The raw materials were provided by Vliegasonie (fly ash) and Orcem (slag). Marija Nedeljkovic provided the X-ray fluorescence results. John van den Berg, Ruud Hendrikx and Hongzhi Zhang helped with the characterization experiments. Telesilla Bristogianni helped with the kiln-casting experiments. Clarissa Justino de Lima is supported by a CNPq (The Brazilian National Council for Scientific and Technological Development) PhD scholarship. They are gratefully acknowledged.

Literature

- Bristogianni, T., Oikonomopoulou, F., Veer, F.A., Snijder, A.H., Nijse, R.: Production and Testing of Kiln-cast Glass Components for an Interlocking, Dry-assembled Transparent Bridge. *Glass Performance Days*, pp 101-106 (2017).
- Bristogianni, T., Oikonomopoulou, F., Justino de Lima, C., Veer, F., Nijse, R.: Cast Glass Components out of recycled glass: potential and limitations of upgrading waste to load-bearing structures. *Challenging glass conference proceedings*, v.6., pp 151-174 (2018).
- Chorfa A., Madjoubi, M.A., Hamidouche, M., Bouras, N., Rubio, J., Rubio, F.: Glass hardness and elastic modulus determination by nanoindentation using displacement and energy methods *Ceramic-Silikaty*, 54, pp 225-234 (2010).
- Deng, W., Wright, R., Boden-Hookb, C., Bingham, P.A.: Briquetting of waste glass cullet fine particles for energy saving glass manufacture. *Glass Technol.: Eur. J. Glass Sci. Technol. A*, Vol.59 (3), pp 81-91 (2018).
- Dhoble, Y.N., Ahmed, S.; Review on the innovative uses of steel slag for waste minimization. *J. Mater. Cycles Waste Manage.* v. 20, Issue 3, pp 1373-1382 (2018).
- Doi, Y., Maehara, T., Yano, T.: Thermal diffusivity of soda-lime-silica powder batch and briquettes. *Glass Technol.: Eur. J. Glass Sci. Technol. A*, v. 59 (3), pp 92-104 (2018).
- Inaba, S.: United States patent application publication. Anisotropic glass. Pub. No.: US 2016/0362328A1 (2016).
- de Jong, B. H. W. S., Glass, in "*Ullmann's Encyclopedia of Industrial Chemistry*"; 5th edition, v. A12, VCH Publishers, Weinheim, Germany, (1989).
- Hendriks, C.A., Worrel, L., Price, L., Martin, N., Ozawa Meida, L., de Jager, D., Riemer, P.: Emission reduction of greenhouse gases from the cement industry. *Proceedings of the 4th International Conference on Greenhouse Gas Control Technologies*, Interlaken, Austria, Aug. 30-Sept. 2, IEA GHG R&D Programme, UK (1998).

- Hoornweg, D., Bhada-Tata, P., Kenney, C.A.: Peak Waste: When Is It Likely to Occur?. *Journal of Industrial Ecology*, 19: pp 117–128 (2015).
- Karamanova, E., Avdeev, G., Karamanov, A.: Ceramics from blast furnace slag, kaolin and quartz. *J. Eur. Ceram. Soc.* v.31, Issue 6, pp 989-998 (2011).
- de Lima, C.J., Veer, F., Çopuroglu, O., Nijssse, R.: Innovative Glass Recipes Containing Industrial Waste Materials. *Challenging Glass Conference Proceedings*, v. 6. pp 533-542 (2018).
- Mauro, J.C.: Decoding the glass genome, *Curr. Opin. Solid State Mater. Sci.* (2017).
- Neupane, K.: Fly Ash and GGBFS Based Powder-Activated Geopolymer Binders: A Viable Sustainable Alternative of Portland Cement in Concrete Industry. *Mechanics of Materials*, 103, pp. 110–122 (2016).
- Paul, A. Chemical Durability of Glass. *Chemistry of Glasses*, Springer. pp 108-147 (1982).
- Rao, G.V., Shashikala, H.D.: Optical and mechanical properties of calcium phosphate glasses. *Glas. Phys. Chem*, 40, pp 303-309 (2014).
- Rosales-Sosa, G.A., Masuno, A., Higo, Y., Inoue, H. Crack-resistant Al₂O₃-SiO₂ glasses. *Scientific Reports* 6, 23620 (2016).
- Rumble, J.R.: *CRC Handbook of Chemistry and Physics*, 98th Edition (Internet Version 2018 <http://hbcponline.com>, CRC Press/Taylor & Francis, Boca Raton, FL, (2017). Accessed 11 January 2018.
- Strachan, D.M., Turcotte, R.P., Barnes, B.O.; MCC-1: A Standard leach test for nuclear waste forms, *Nuclear Technology*, v.56, Issue 2, pp 306-312 (1982).
- WMO Greenhouse Gas Bulletin no.13: The State of Greenhouse Gases in the Atmosphere Based on Global Observations through 2016, (2017).
- Zanotto, E.D., Coutinho, F.A.B.: How many non-crystalline solids can be made from all the elements of the periodic table?, *J Non-Cryst. Solids* 347, pp 285–288 (2004).
- Zhang, J., Dong, W., Li, L., Qiao, L., Zheng, J., Sheng, J.; Utilization of coal fly ash in the glass-ceramic production. *J. Hazard. Mater.* v. 149, Issue 2, pp 523-526 (2007)
- Zschimmer, E.: *Chemical technology of glass*. Sheffield: Society of Glass Technology (2013).

